Featured Article

Linking the low-density lipoprotein receptor-binding segment enables the therapeutic 5-YHEDA peptide to cross the blood-brain barrier and scavenge excess iron and radicals in the brain of senescent mice

Zhenyou Zou[a,b,c,*,1], Shengxi Shao[d,1], Ruyi Zou[e,1], Jini Qi[b,1], Liguan Chen[f,1], Hui Zhang[g,1], Qiqiong Shen[b,1], Yue Yang[h,1], Liman Ma[b,1], Ruzeng Guo[b,1], Hongwen Li[a,1], Haibo Tian[a,1], Pengxin Li[a], Mingfang Yu[a], Lu Wang[a], Wenjuan Kong[a], Caiyu Li[a], Zhenhai Yu[a], Yuping Huang[a], Li Chen[a], Qi Shao[b], Xinyan Gao[b], Xiaolin Chen[b], Zhengbo Zhang[b], Jianguo Yan[a], Xiaoyun Shao[a], Ru Pan[a], Lu Xu[i], Jing Fang[b], Lei Zhao[e], Yaohui Huang[e], Anqi Li[b], Yuchong Zhang[b], Wenkao Huang[b], Kechun Tian[b], Minxin Hu[b], Linchao Xie[b], Lingbin Wu[b], Yu Wu[b], Zhen Luo[b], Wenxin Xiao[b], Shanshan Ma[e], Jianan Wang[e], Kaixin Huang[e], Siyuan He[e], Fan Yang[e], Shuni Zhou[b], Mo Jia[b], Hui Zhang[j], Hongsheng Lu[j], Xinjuan Wang[b,**], Jie Tan[a,***]

[a]Guangxi Key Laboratory of Brain and Cognitive Neuroscience, Guilin Medical University, Guilin, GX, China
[b]Medical School of Taizhou University, Taizhou, ZJ, China
[c]Biochemistry Department, Purdue University, West Lafayette, USA
[d]Division of Cell and Molecular Biology, Imperial College London, London, United Kingdom
[e]Chemistry Engineering Department, Shangrao Normal University, Shangrao, JX, China
[f]Zhejiang Armed Police Corps, Hangzhou, ZJ, China
[g]China Tobacco Gene Research Center, Zhengzhou Tobacco Research Institute of CNTC, Zhengzhou, HN, China
[h]Clinical Laboratory Department, Wenzhou Medical University, ZJ, China
[i]Clinical Laboratory of Jingyou Hospital, Xiaoshan, ZJ, China
[j]Pathology Department, Affiliated Hospital of Taizhou University, ZJ, China

Abstract

Introduction: Iron accumulates in the brain during aging, which catalyzes radical formation, causing neuronal impairment, and is thus considered a pathogenic factor in Alzheimer's disease (AD). To scavenge excess iron-catalyzed radicals and thereby protect the brain and decrease the incidence of AD, we synthesized a soluble pro-iron 5-YHEDA peptide. However, the blood-brain barrier (BBB) blocks large drug molecules from entering the brain and thus strongly reduces their therapeutic effects. However, alternative receptor- or transporter-mediated approaches are possible.

Methods: A low-density lipoprotein receptor (LDLR)-binding segment of Apolipoprotein B-100 was linked to the 5-YHEDA peptide (bs-5-YHEDA) and intracardially injected into senescent (SN) mice that displayed symptoms of cognitive impairment similar to those of people with AD.

Results: We successfully delivered 5-YHEDA across the BBB into the brains of the SN mice via vascular epithelium LDLR-mediated endocytosis. The data showed that excess brain iron and radical-induced neuronal necrosis were reduced after the bs-5-YHEDA treatment, together with cognitive amelioration in the SN mouse, and that the senescence-associated ferritin and transferrin increase, anemia and inflammation reversed without kidney or liver injury.

Discussion: bs-5-YHEDA may be a mild and safe iron remover that can cross the BBB and enter the brain to relieve excessive iron- and radical-induced cognitive disorders.

1. Introduction

Alzheimer's disease (AD) is a progressive neurodegenerative disease of the brain characterized by memory impairment and disturbances in reasoning, planning, language, and perception [1]. The brains of people with AD have numerous amyloid plaques and neurofibrillary tangles in the hippocampus, cortex, and temporal lobe [2]. Currently, AD cannot be cured, and those suffering from AD heavily rely on others for assistance, which places a great burden on their caregivers and society [3].

The cause of AD is not well understood. Many studies have demonstrated that increased oxidative stress levels in the brain may play a pathogenic role in neuronal degeneration because oxidative radicals impair membrane lipids and proteins, which can lead to neuronal destruction [4,5].

Iron, as a transition metal, can catalyze free oxidative radical generation by deoxidizing oxygen to oxyradicals or by donating electrons to hydrogen peroxide, forming hydroxyl radicals [6]. It has been reported that iron can accumulate regionally with aging because of changes in iron-metabolic protein localization during development [7], and the iron distribution determines the regional density of radicals and the injury severity [7]. Therefore, reducing excess iron in the brain may be an option for alleviating AD.

Metal chelators, such as deferoxamine (DFO) and deferiprone (DFP), have been used to treat AD in clinical trials [8–12]. These agents have slowed the progression of AD in specific cases [9,12]. However, fundamental aspects of the biochemistry of these agents have severely limited their effectiveness. For example, the hexadentate iron chelator DFO can tightly bind iron(III) to impede the progression of AD [13–15]. The lipid-soluble iron chelator DFP is known to lower the neutrophil and white blood cell count and cause life-threatening infections [16,17]. Therefore, a nontoxic iron chelator that removes excessive iron from the brain must be identified or designed.

Amyloid beta (Aβ) is a 36 to 43 amino acid peptide present in organisms that is cleaved from amyloid precursor protein by beta secretase [18]. Aβ has a high affinity to Cu^{2+} and Fe^{3+} and can bind iron ions at Asp $(D)_1$, Glu $(E)_3$, and His $(H)_{6,13,14}$ sites; this property enables it to reduce excessive iron in the cerebrospinal fluid (CSF) [19–23]. However, because of its low solubility and the potential malignant effects of radical catalysis by the Aβ peptide, we combined these metal pro–amino acid Asp (D), Glu (E), and His (H) residues to form a new amino acid oligomer. Furthermore, to enhance the solubility of the oligomer, we added polar amino

acid tyrosine (Y) and the smallest nonpolar amino acid alanine (A) with the aim of chelating excess iron and decreasing radicals in the brain to ease AD symptoms.

However, the blood-brain barrier (BBB), which is formed by endothelial cell tight junctions, hampers molecules >500 Da from entering the brain, thereby severely inhibiting their therapeutic efficiency [24]. Various methods for transporting drugs across the BBB have been investigated. Several receptors present in the BBB, including transferrin, the insulin receptor, and the low-density lipoprotein receptor (LDLR), are known to allow the passage of cognate protein ligands into the brain [25–27]. LDLR-related protein is a multifunctional endocytic receptor that mediates the endocytosis of multiple ligands. This protein can also be expressed on the membrane of the cells in the BBB and has been used to develop strategies for delivering drugs to their targets [28]. Apolipoprotein B-100 (ApoB-100) is a lipid carrier. When recognized and bound by LDLR at the BBB, the complex can be converted to an endosome, subsequently resulting in transcytosis to the abluminal side of the BBB. There, the apolipoprotein can be released for uptake by neurons and/or astrocytes when the pH is reduced, and the receptor is recycled to the cell surface [29].

Lipid-interactive regions and LDLR-binding regions are scattered in ApoB-100. The primary LDLR-binding region is located between amino acids 3359 and 3367, which consists of nine amino residues with the sequence "QSDIVAHLL" [30]. To facilitate transport of the therapeutic YHEDA peptide across the BBB, we added the aforementioned LDLR-binding segment in ApoB-100 to the C-terminal of the synthesized therapeutic 5-YHEDA oligomer. Using this method, we intended to deliver 5-YHEDA into the brains of senescent (SN) mice via LDLR-mediated endocytosis and allow it to function as an excess brain iron scavenger.

Many animals will experience iron accumulation during aging, which causes neuronal degeneration and cognitive impairment [7]. To carry out our study, we used the Morris water maze (MWM), TdT-mediated dUTP nick end labeling (TUNEL) assay, and routine blood assays to identify 58 naturally SN mice among fifteen hundred 25-month-old Kunming mice. The identified SN mice displayed memory and cognitive impairment, neuronal necrosis, and inflammation, which are very similar to the symptoms displayed by human patients with AD. In particular, the iron level in the brain of the SN mouse is higher than normal (shown in Fig. 1A), which suggests that this model is very suitable for examining the changes in iron and radicals in the brain and the damage they cause. To verify the effectiveness of
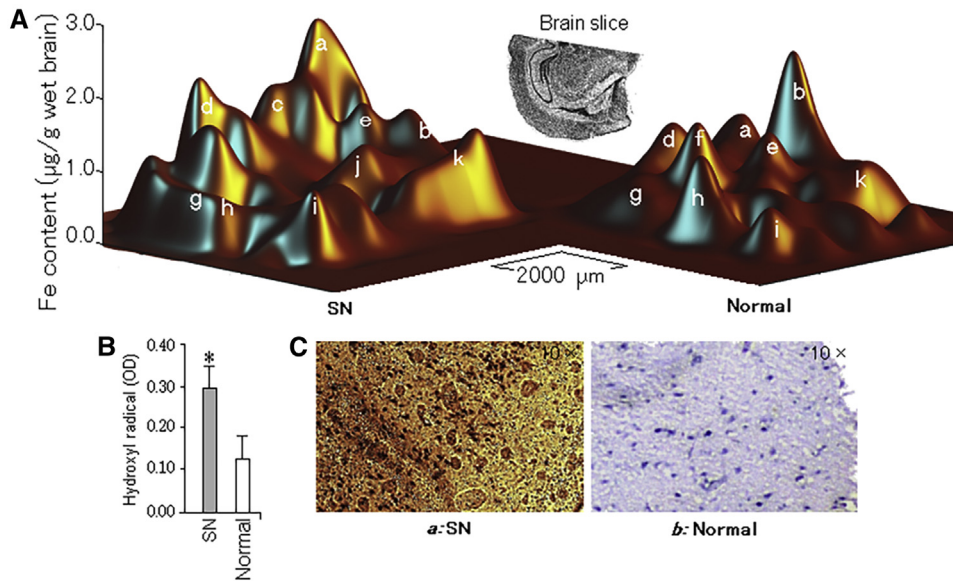
Fig. 1. The SN mouse brain is rich in iron and radicals and exhibits widespread necrotic neurons. (A) The SN mouse brain has more iron than the normal brain. The average iron level in the SN brain is 0.72 μg per gram wet brain, which is highly concentrated in the corpus callosum, cortex, hippocampus, lateral preoptic area, cingulate cortex, and amygdala of the AD brain but scarce in the ventricles, prerubral field, and lateral entorhinal cortex. In contrast, the normal brain has only 0.43 μg per gram wet brain. (a) Indusium griseum-retrosplenial granular b cortex; (b) dorsal third ventricle; (c) parietal association cortex; (d) primary somatosensory cortex, barrel field; (e) lateral posterior thalamic nucleus, mediorostral part; (f) field CA1-CA3 of hippocampus; (g) temporal cortex; (h) perirhinal cortex-lateral entorhinal cortex; (i) amygdala; (j) thalamus; and (k) hypothalamus. (B) The hydroxyl radical is abundant in the brains of SN mice, nearly 140% higher than that of normal mice. (C) The brown spots stained by TUNEL-DAB in SN mouse brain slices show that the necrotic neurons are widespread in SN brains. *$P < .05$. Abbreviations: AD, Alzheimer's disease; DAB, 3,3′-diaminobenzidine; SN, senescent; TUNEL, TdT-mediated dUTP nick end labeling.

the binding segment–containing 5-YHEDA peptide (abbreviated as bs-5-YHEDA) in iron and radical elimination and neuron-protection, we delivered the synthesized bs-5-YHEDA to the SN mice via cardiac injection and evaluated the aftermath.

2. Materials and methods

2.1. Materials

The 5-YHEDA and bs-5-YHEDA amino acid oligomers were synthesized by GL Biochem Ltd (Shanghai, China). The human neuroblastoma cell line SH-sy5y and human vascular endothelial cell line HECV were obtained from American Type Culture Collection (ATCC, Manassas, VA). The Kunming mice were provided by the Animal Center of Wenzhou Medical University (Wenzhou, China). Fifty-eight naturally aging mice (25 months old) that displayed poor learning (escape latency >75 s) in the MWM and later immunohistochemically detected dense necrotic neurons (>2/mm^2) in the corpus callosum and hippocampus were used to investigate the therapeutic efficiency of 5-YHEDA or bs-5-YHEDA in the pathology of senescence.

2.2. Brain iron content topography scanning and measurement

Six normal or SN mice were executed after anesthetized with pentobarbital dissolved in saline (70 mg/kg mouse),

and the brains were removed and coronally frozen-sectioned (20 μm thick) according to Fig. 30 of Reference [31]. Three sections of each brain were placed on a polycarbonate membrane after weighing, and the sections were scanned using an X-fluorescence workstation (Institute of High Energy Physics, Beijing, China) for iron topography. Other sections from the same brain were reserved for TUNEL or immunocolloidal gold assay.

The iron levels in the brain and CSF were measured using six other normal or SN mice. Along with cell culture medium, all samples were measured by an inductively coupled plasma emission spectrometer (PerkinElmer Elan600, Fremont, CA). Before the measurements, the samples were individually freeze-dried, weighed, and nitrified. CSF was extracted from the ventricle of each subject using stereotaxic coordinates of PA-1.0 mm, lateral-1.5 mm from the bregma, and ventral-2.0 mm relative to the dura. Gradient concentration FeCl$_3$ solutions were used as standards.

2.3. Transmission electron microscopy observation on 5-YHEDA chelation of iron and agglomeration

The synthesized 5-YHEDA powder was dissolved in distilled water (1 mg/mL) and then divided into two aliquots. The first was used as the control, without the addition of iron. In the second aliquot, 5 μL 0.01 M FeCl$_3$ solution was added to 20 μL 5-YHEDA lyosol and then incubated for 3 hours at 37°C. Next, each sample was placed on a carbon film-coated

copper mesh and exposed to 2 minutes of 1% (w/v) phospho-tungstic acid staining. The samples were air-dried and then observed under a transmission electron microscope (H7650, Hitachi, Kyoto) equipped with an EMAX X-ray energy spectrometer (Horriba, Kyoto, Japan) to detect the iron distribution.

2.4. Isothermal titration calorimetry

To confirm the affinity between the iron atoms and 5-YHEDA, purified 5-YHEDA oligomers were exhaustively dialyzed against the isothermal titration calorimetry (ITC) buffer. Then, the 5-YHEDA oligomers were diluted to 200 μM, and the $FeCl_3$ was diluted to 1000 μM. The binding between iron and 5-YHEDA oligomers was measured using a VP-ITC microcalorimeter (MicroCal, GE Healthcare). The heat of the ligand dilution was subtracted from the heat of the binding to generate a binding isotherm that was fit with a one-site binding model using origin, allowing the association constant (K_a), enthalpy (ΔH), and entropy (ΔS) of the interaction to be determined. K_a was used to calculate K_d ($K_d = 1/K_a$).

2.5. Infrared spectrum analysis

To determine how 5-YHEDA binds iron ions, dried 5-YHEDA:$FeCl_3$ reactant was blended with K_2Br powder (1:5), and the infrared (IR) spectra of the samples were triply measured using an IR spectrometer (NEXUS870, NICOLET). Pure 5-YHEDA and K_2Br were used as the controls.

2.6. Cell culture

SH-sy5y cells were cultured in Roswell Park Memorial Institute Dulbecco's Modified Eagle Media at 37°C under 5% CO_2 for 12 hours and then divided into iron-stress, iron + 5-YHEDA, and iron + bs-5-YHEDA groups (each group containing three dishes of cells). In the iron-stress group, 0.01 mM $FeCl_3$ was added to mimic the levels in the AD brain CSF, and the remaining two groups were supplemented with 0.01 mM $FeCl_3$, but with 1.5 μM 5-YHEDA or bs-5-YHEDA also added to the medium. The peptide concentration was optimized beforehand. The groups with/without 5-YHEDA or bs-5-YHEDA were set as the controls. All plates of cells were cultured for 12 hours. Then, some of the cells in each dish were fixed with 2.5% glutaraldehyde for scanning electron microscopy; the remaining cells were used in flow cytometry for an apoptosis assay (BD FACSCalibur, Franklin Lake). The medium in each dish was individually collected for radical and iron measurements.

Human vascular endothelial cells (HECV) were cultured under the same conditions for the LDLR:bs-5-YHEDA coimmunoprecipitation assay.

2.7. Cell apoptosis assay

SH-sy5y cells in different dishes were individually collected and stained with annexin-V–fluorescein isothiocyanate and propidium iodide for 10 minutes in the dark at room temperature. A FACScan flow cytometer (Becton Dickinson and Company) was used to analyze cell apoptosis. CellQuest Pro software (Becton Dickinson Company) was used to determine the percentage of the total cells that were apoptotic.

2.8. Hydroxyl radical measurement

The CSF of each mouse brain (50 μL for each), along with the same volume of cell culture medium from each dish, was individually placed in 50 μL 1% salicylic acid solution (w/v). After the samples were incubated on a shaker at 37°C for 15 minutes, they were submitted for analysis of transmittance at the 510 nm wavelength using an enzyme-labeled meter (SpectraMax M5, Molecular Devices). The optical density value was set to measure the hydroxyl radical level in each sample.

2.9. Anti–5-YHEDA immune serum preparation

One hundred microliters of 5-YHEDA–physiological saline (0.1 mg/mL) was mixed with 100 μL of incomplete Freund adjuvant and then subcutaneously or intraperitoneally injected into normal mice weekly. After 2 months, the whole blood of each mouse was extracted, and the serum was isolated and frozen at −20°C for later use.

2.10. Coimmunoprecipitation

HECV were cultured under standard conditions. When the density reached 5×10^6 cells/dish, the cells were washed three times with ice-cold phosphate-buffered saline (PBS) and lysed on ice using a 100 μL nondenaturing lysis solution containing a protease inhibitor cocktail. A solution containing bs-5-YHEDA or 5-YHEDA peptide (100 μg/mL) was mixed with the lysate, and then monoclonal anti-LDLR was added to the protein lysate and incubated for 3 hours at 4°C. The protein A/G agarose was then coincubated overnight, and the purified protein complexes were recovered via centrifugation and heated to 95°C for 5 minutes.

2.11. Western blotting

Ten percent sodium dodecyl sulfate–polyacrylamide gel electrophoresis was selected to separate samples (20 μg) containing equal amounts of protein, after which the samples were transferred to a nitrocellulose membrane. The membranes were washed with Tris-buffered saline with 0.1% Tween 20 four times (5 minutes for each wash) at room temperature. Next, the membranes were blocked with 1% bovine serum albumin and then incubated with antibodies (anti–5-YHEDA serum was used to detect the coimmunoprecipitation of LDLR and bs-5-YHEDA; antiferritin or

antitransferrin immunoglobulin G was used to detect the expression of ferritin or transferrin in the brain) at 4°C overnight. The next day, after five PBS washes, the membrane was incubated with horseradish peroxidase-labeled secondary antibody for 2 hours at room temperature. Then, the bound antibodies were detected using enzyme-linked chemiluminescence (Pierce Biotechnology, Inc, Chicago, IL). Glyceraldehyde-3-phosphate dehydrogenase was used as an internal control for the loading and standardization of the samples. Each experiment was repeated three times.

2.12. Dose-dependent and duration-effect investigation

To evaluate the efficiency of bs-5-YHEDA on brain protection, dose-dependent and duration-effect investigations were performed. In the dose-dependent test, 200 μL of 0.0, 0.5, 1.0, 5.0, 20, or 40 μM physiological saline dissolved bs-5-YHEDA was intracardially injected into each mouse in groups weekly. After 4 weeks, 50 μL CSF was extracted from the ventricle of each subject.

In the duration-effect experiment, each mouse was intracardially injected with 200 μL of 20 μM bs-5-YHEDA weekly according to a time table. Fifty microliters of CSF was extracted from each mouse, and then the hydroxyl radical in the CSF was measured with salicylic acid.

2.13. Brain bs-5-YHEDA bioavailability assay by quantitative autoradiography

Forty-eight hours after the cardiac injection of 200 μL 20 μM ^{3}H-bs-5-YHEDA, the normal mouse brains were frozen-sectioned into 20 μm coronal slices. Along with a series of freeze air-dried gradient concentration ^{3}H-bs-5-YHEDA solution droplets on another slide (used to quantitate the bioavailability of the ^{3}H-bs-5-YHEDA in brain slices), the brain slices pasted on a glass slide were then placed in an X-ray cassette that contained ^{3}H-sensitive autoradiography film (Leica Inc, Deerfield, IL). After exposure for 2 weeks at room temperature, the autoradiography film was then developed and fixed. Then, the films were digitized to produce digital images. The tritium activity at each pixel location was used to present the bioavailability of the bs-5-YHEDA peptide distributed in the brain. The freeware program National Institutes of Health-Image (written by Wayne Rasband; available by anonymous FTP from zippy.nimh.nih.gov) was used to measure concentration profiles from individual digital images. Local concentrations obtained by this method are expressed in radioactivity units (nCi/mg)

2.14. 5-YHEDA immunohistochemical staining

Fixed brain slices were blocked with 0.1% bovine serum albumin/PBS (w/v). One hour later, anti–5-YHEDA serum was added to the sections. The sections were incubated at 4°C overnight and then washed. Horseradish peroxidase-labeled goat anti-mouse immunoglobulin G was then incu-

bated with the sections. After 2 hours, the samples were washed again and then covered by the enzyme 3,3′-diaminobenzidine. After 30 minutes, the sections on the slides were stained with hematin. The samples were washed three times with PBS and observed under a microscope. The sections that contained scattered brown spots were positive for 5-YHEDA, indicating that 5-YHEDA reached the brain.

2.15. MWM test

The MWM was used to evaluate the learning and memory ability of the mice. The water maze was 1.5 m in diameter and 0.6 m in depth and filled with milk beforehand. In the center, there was a stage 1 cm under the liquid. In the experiment, the SN Kunming mice exhibiting AD symptoms were divided into untreated, 5-YHEDA–treated, and bs-5-YHEDA–treated groups. Two hundred microliters of 20 μM 5-YHEDA or bs-5-YHEDA solution was intracardially injected into each mouse in the latter two groups weekly. The 6-month-old mice and the aging mice that did not display SN symptoms were used as the controls. Six weeks later, all mice underwent a 4-day MWM test after 1 day of adaptation. The path that the mouse swam to return to the underwater platform and the time spent were recorded to evaluate the individual's cognitive ability.

2.16. Functional brain magnetic resonance imaging assay

The brain oxygen metabolism level in the mice was observed using a nuclear magnetic resonance spectrometer (E40, Flir Inc) at 1.5 T for 30 minutes after the mice were anesthetized. The signal intensity in the brain determined the oxygen metabolism level.

2.17. Hematologic analyses

To evaluate the side effects of bs-5-YHEDA, mouse blood was collected according to the International Association of Clinical Chemistry Committee on Reference Intervals and Decision Limits protocol [32]. One milliliter of venous blood was drawn into a vacuum tube containing potassium 2 ethylenediaminetetraacetic acid. Hematologic analyses were performed to evaluate the white blood cell count, neutrophil percentage, lymphocyte percentage, monocyte percentage, basophil percentage, eosinophil percentage, red blood cell count, hematocrit, mean corpuscular volume, mean corpuscular hemoglobin concentration, red cell distribution width, platelet count, and mean platelet volume.

2.18. Clinical chemistry

Clinical chemistry was performed to determine the side effects of bs-5-YHEDA on the kidney or liver. Specifically, blood urea nitrogen was assayed using a SpectraMax microtiter plate reader (Molecular Devices, LLC) and a MaxDiscovery Blood Urea Nitrogen Enzymatic Kit (Bioo Scientific Corporation). The Quantichrom Creatinine Assay

Kit (BioAssay Systems) was used to measure creatinine in the serum. The serum activity of aspartate aminotransferase and alanine aminotransferase was determined using an automated analyzer (Selectra Junior Spinlab 100, Vital Scientific, Dieren, Netherlands) according to the manufacturer's instructions.

2.19. Colloidal gold immunohistochemical staining and iron:bs-5-YHEDA colocalization scanning

To determine whether iron binds to the bs-5-YHEDA peptide in vivo, a colloidal gold immunohistochemical scanning electron microscope (SEM) scan was performed. The brain slices were immunohistochemically stained with the anti–5-YHEDA mouse serum and then incubated with a colloidal gold–labeled immunoglobulin G solution immediately after the wash. After incubation for 2 hours at room temperature, the samples were washed and freeze-dried with *tert*-butanol. After being vacuum-sputtered with gold particles, the samples were observed under an SEM (S-3000N, Hitachi, Kyoto). The iron distribution in each slice was scanned using the x-ray energy spectrum (EX-450, HORIBA EMAX, Japan) equipped to the SEM, and the iron:bs-5-YHEDA colocalization topography was acquired simultaneously.

2.20. TUNEL assay

Cell necrosis in the brain was assessed using a TUNEL kit (Sangon Biotech Inc Shanghai, China). Briefly, frozen mouse brain sections were incubated in Na-N-2-hydroxyethylpiperazine-N-ethane sulphonic acid solution for 1 hour and then treated with $10\,mM\,H_2O_2$ and 20 mM progesterone. After washing in PBS and then permeabilizing with 0.1% Triton-X 100, a TUNEL reaction mixture incubation was performed for 1 hour at 37°C in the dark. Parts of the specimens were subsequently stained with 3,3′-diaminobenzidine. Then, the samples were observed with microscopy. Bright or brown spots indicated necrotic cells in the tissue.

2.21. Data processing

Each sample was measured three or more times, and the data are presented as the mean ± standard error of the mean. The differences were considered statistically significant at $P < .05$ using t tests.

3. Results

3.1. The SN mouse brain has higher levels of iron and hydroxyl radicals and overt neuronal necrosis

The brain of the SN mouse had more iron than that of the normal mouse, exhibiting 0.72 μg iron per gram on average, whereas the normal mice had only 0.43 μg per gram (Fig. 1A). In more detail, the topography (Fig. 1A) showed that the iron was highly concentrated in the corpus callosum, cor-

tex, hippocampus, lateral preoptic area, cingulate cortex, and amygdala of the AD brain (Fig. 1A-a, c, d, e, g, i, j) but was scarce in the ventricles, prerubral field, and lateral entorhinal cortex (Fig. 1A-b, h). In contrast, the iron levels were relatively low in most areas of the normal brain, except for sporadic densities in the ventricles (Fig. 1A-b) and CA1 (adjacent to Fig 1A-b).

Accordingly, in the SN brain, the hydroxyl radical (●OH) level was 140% higher than that of the normal brain (Fig. 1B), and necrotic neurons (brown spots in Fig. 1C-a) were widespread.

3.2. 5-YHEDA can bind iron

Mass spectrometry (Fig. 2A) showed that the particles with five hydrions appeared at *m/z* peak 715.85, which is the molecular weight (MW) of a one-repeat "YHEDA" oligomer. The left peak, 630.11, is the oligomer "YHED", which being the fragment of YHEDA lost an alanine (MW = 89) and several hydrogen atoms. The four-hydrion particles and three-hydrion particles were, respectively, located at 894.81 *m/z* and 1192.40 *m/z*. They are the fragment "YHEDA-Y" and "YHEDA-YHE" oligomers (the MWs of Y, H, E, and D are 181, 155, 147, and 133, respectively). Therefore, the MW of the whole synthesized oligomer is 3574.5, which accounts for five repeats of YHEDA. More information about the peptide can be derived from an intensive analysis of the weak peaks scattered along the spectrum.

Using a protein sequencer (PPSQ-21A/23A, Shimadzu Corp, Japan), the peptide oligomer was sequenced as "YHEDA YHEDA YHEDA YHEDA YHEDA," and the LDLR-binding segment containing oligomer was sequenced as "YHEDA YHEDA YHEDA YHEDA YHEDA-QSDI-VAHLL." The segment highlighted in gray is the LDLR-binding amino acid sequence, which completely conformed to our design.

The 5-YHEDA oligomer is approximately 150 nm in length (Fig. 2B-c) and displays a linear-like fibril but can be curled and conglomerated after incubation with $FeCl_3$ (Fig. 2B-d); the iron (the bright spots in the right panel of Fig. 2B-d) was isodirected along the 5-YHEDA fibrils, strongly suggesting that junctions appeared between the iron atoms and the amino acid oligomers after mixing and incubation. ITC confirmed the affinity. As shown in Fig. 2C-b, after the $FeCl_3$ titration, the 5-YHEDA lost 91,255 kcal/mol in enthalpy and 8973 kcal/mol in Gibbs energy. In contrast, very little heat was released when 5-YHEDA was titrated using the ITC buffer (Fig. 2C-a, each titration released 0.26 kcal/mol or less). More in-depth, IR chromatography showed that the 5-YHEDA oligomer binds iron at residues His, Tyr, Asp, and Glu. The peaks in the band of 1600 to $1300\,cm^{-1}$, which represent the C]O group vibrations in the carboxyl groups of Glu and Asp, were changed after incubation with $FeCl_3$. The peak at $720\,cm^{-1}$, which represents the weakening of the phenyl hydroxide of Tyr (Fig. 2D-b); the absorption apex at $2375\,cm^{-1}$, which represents the stretching of the C–N bond; and the peaks in the
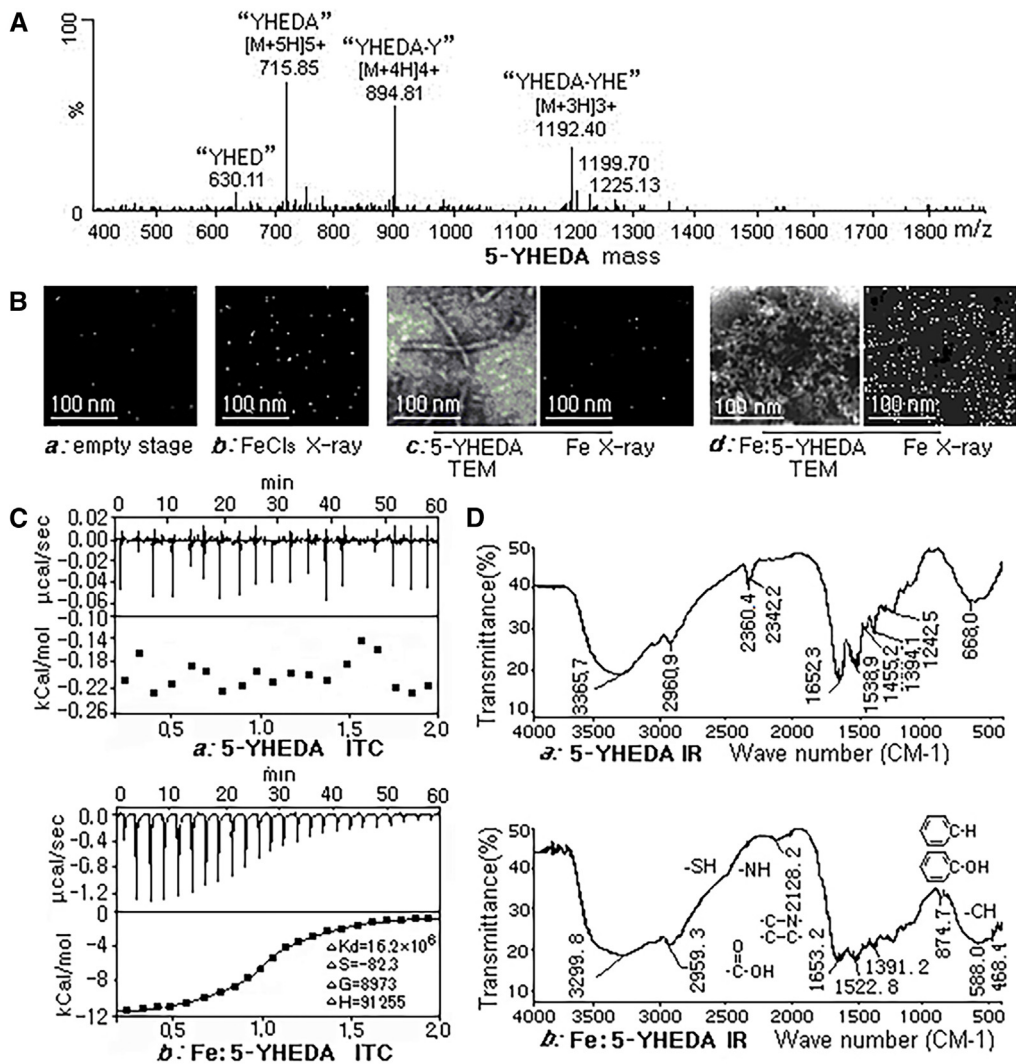
Fig. 2. 5-YHEDA shows affinity for iron ions. (A) Mass spectrum of the synthesized 5-YHEDA amino acid oligomer. The site $m/z = 715.85$ represents the particles with five hydrions. It is a one-repeat "YHEDA" oligomer. Peak 630.11 is the "YHED" oligomer, which is the fragment of YHEDA that has lost an alanine and several hydrogen atoms; peaks 894.81 and 1192.40 are the sites of four-hydrion and three-hydrion fragments, respectively. They are the "YHEDA-Y" and "YHEDA-YHE" oligomers. On these grounds, the molecular weight of the whole peptide is 3574.5. (B) TEM images of 5-YHEDA oligomers with or without $FeCl_3$ incubation. The $FeCl_3$ incubation resulted in the agglomeration of the 5-YHEDA oligomer, and the x-ray energy spectrum shows iron isodirected along the amino acid fibril. (C) ITC indicates that the enthalpy of the Fe:5-YHEDA compound lost 91,255 kcal/mol enthalpy and 8973 kcal/mol Gibbs energy, indicating that 5-YHEDA has a higher affinity for iron. (D) Infrared spectra of 5-YHEDA before and after $FeCl_3$ incubation. The signal at $720 \, cm^{-1}$, which could be assigned to the phenyl-OH in the Tyr residue; the signal at $2925 \, cm^{-1}$, and the peaks in the band of 1600 to $1300 \, cm^{-1}$, which could be assigned to the –COOH in the residues of Glu or Asp; and C–N ($2375 \, cm^{-1}$) and C=N ($700–1615 \, cm^{-1}$) in the His residue were all weakened, suggesting that iron binding occurred. Furthermore, the signals representing the backbone acrylamide N–H stretching ($3500–3100 \, cm^{-1}$), the C=O bond shift ($1680–1630 \, cm^{-1}$), the N–H bending ($1655–1590 \, cm^{-1}$), and C–N stretching ($1420–1400 \, cm^{-1}$) were transformed, indicating that tortuosity occurred in the backbone after iron incubation. Abbreviations: ITC, isothermal titration calorimetry; TEM, transmission electron microscope.

1700 to $1615 \, cm^{-1}$ band, which represent the stretching of the C]N bond in the imidazole ring of the histidine residue, were all weakened (Fig. 2D-b) after the $FeCl_3$ incubation. These results suggest the possibility of iron-atom chelation.

3.3. 5-YHEDA and bs-5-YHEDA can protect cells by reducing radicals

Iron ions can catalyze radical production. If it occurs in the brain, neurons will be impaired, resulting in a decrease in number and dysgnosia. To confirm that 5-YHEDA or bs-5-YHEDA can protect neurons against damage caused by iron-catalyzed radicals, we administered the synthesized 5-YHEDA or bs-5-YHEDA to the iron-rich (containing 15 μM $FeCl_3$, imitating AD CSF) medium cultured neuroblastoma cell SH-sy5y. Before the treatment, we measured the efficiency of the YHEDA repeats on iron binding and hydroxyl reduction to obtain an optimal peptide length and an appropriate dose. As shown in Fig. 3A, with the repeat increase in YHEDA, the efficiency of iron chelation and
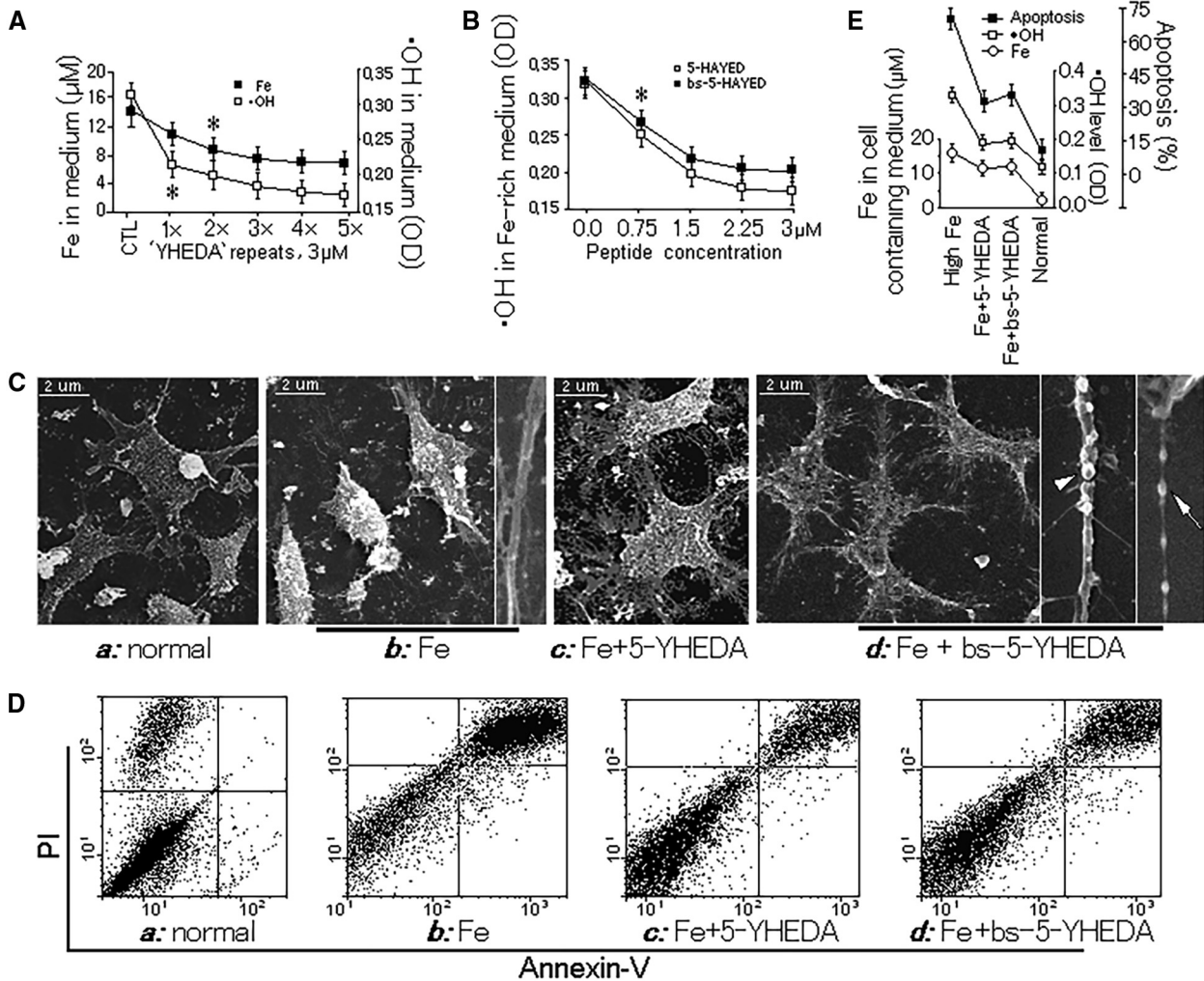
Fig. 3. 5-YHEDA and bs-5-YHEDA protect cells in vitro by reducing iron and hydroxyl radicals. (A) The more "YHEDA" repeats a peptide has, the more effective the peptide is at reducing iron and hydroxyl radicals. (B) Iron decreases with increasing density of 5-YHEDA. Although linked to the LDLR-binding segment, 5-YHEDA can still effectively reduce the radicals in the iron-rich medium, although the binding segment "QSDIVAHLL" diluted the residues with iron affinity to and thus probably slightly weakened the radical-eliminating ability. (C) The SH-sy5y cells shrank in the iron-rich medium, the dendritic spines (arrowhead) decreased, and axonal transportation (arrow) disappeared. In contrast, in the 5-YHEDA or bs-5-YHEDA–supplemented high-iron medium, the cells survived, their axons and dendrites extended, their dendritic spines increased, and the cytoplasmic transportation was active. Transporting cysts were observed along the dendrites. (D and E) Flow cytometry and iron-•OH radical assays demonstrated that both 5-YHEDA and bs-5-YHEDA peptides decreased hydroxyl radicals and iron in the medium, resulting in increased cell survival. *$P < .05$. Abbreviations: LDLR, low-density lipoprotein receptor; PI, propidium iodide.

hydroxyl scavenge increased until the length increased to four repeats, and the effects increase slowed down. Therefore, we added the 5-repeat YHEDA or bs-5-YHEDA oligomer to the medium and observed that the number of radicals in the medium also decreases with the oligomer density (Fig. 3B).

When the 5-YHEDA or bs-5-YHEDA peptide was added to the iron-rich medium with SH-sy5y cells in culture, both peptides protected the cells (Fig. 3C–E). Spectrophotometry and inductively coupled plasma assays revealed that after 36 hours, the hydroxyl radicals in the medium decreased from 0.34 to 0.19, and the free iron ions in the medium decreased by one-third (Fig. 3E). Particularly, many of the SH-sy5y cells cultured in iron-rich medium survived when

added to 1.5 μM 5-YHEDA or bs-5-YHEDA, their axons and dendrites were intact, and the spines on their dendrites were abundant (indicated by the arrowhead in Fig. 3C-d). Furthermore, the cells exhibited active cytoplasmic transportation, as demonstrated by transporting cysts observed along the dendrites (indicated by the arrow in Fig. 3C-d). In contrast, without 5-YHEDA or bs-5-YHEDA, the cells in iron-rich medium atrophied, their axons and dendrites shrank, and the number of dendritic spines decreased (Fig. 3C-b). No transporting cysts were observed (Fig. 3C-b), suggesting that iron stress impairs the physiological activities of the cell but that 5-YHEDA or bs-5-YHEDA can exempt the stressed cells from a hazard environment full of free radicals.
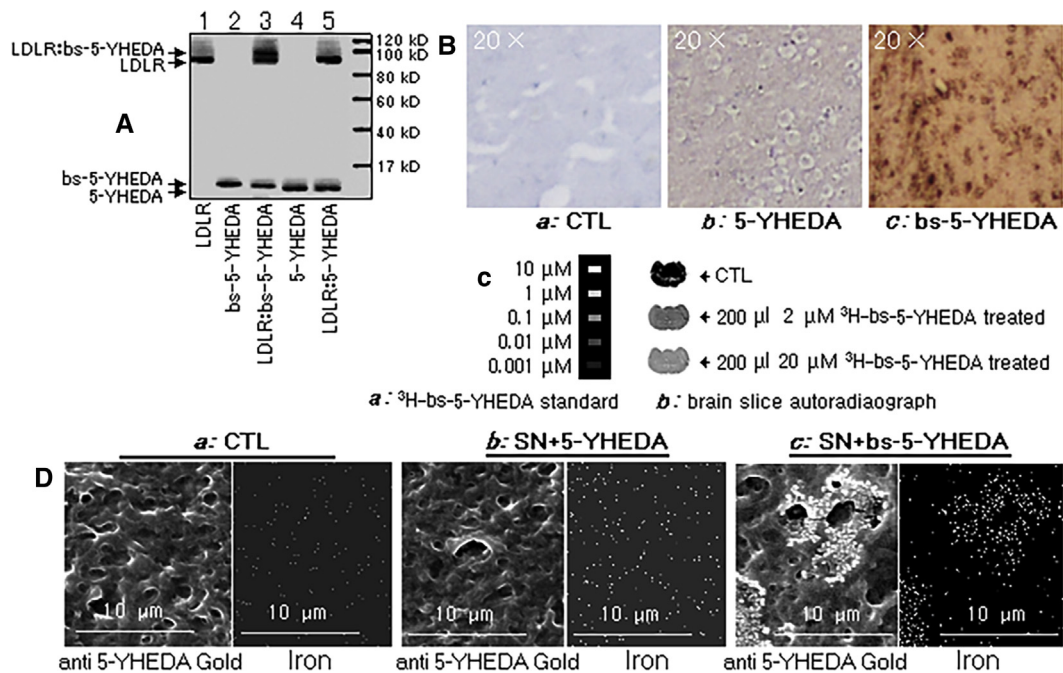
Fig. 4. LDLR-binding segment enables 5-YHEDA to cross the BBB and enter the brain. (A) At the level of 100 kDa, there is a bold black band above LDLR in lane 3, with nearly the sum MWs of bs-5-YHEDA and LDLR, which is the complex of bs-5-YHEDA:LDLR. In contrast, in lane 5, the mixture of 5-YHEDA and LDLR electrophoresed to two independently thick black bands. One was at the same level as LDLR, and the other ran to the bottom. In this lane, no band thicker than the 100 kDa compound was found, suggesting that 5-YHEDA scarcely interacts with LDLR. (B) Immunohistochemistry shows that linking an LDLR-binding segment to 5-YHEDA enabled the peptide to cross the BBB and enter the brain. (a and b) The control and 5-YHEDA cardiac-injected brain sections exhibited no staining, (c) but in the bs-5-YHEDA cardiac-injected mouse brain, there were scattered anti–5-YHEDA serum stained brown blots, which might indicate that the bs-5-YHEDA crossed the BBB and entered the brain. (C) ^{3}H-bs-5-YHEDA autoradiography shows that after 6 days of cardiac injection with 200 μL 20 μM ^{3}H-bs-5-YHEDA, the concentration of the remaining ^{3}H-bs-5-YHEDA in the brain was approximately 0.26 μM, which is still an active concentration. (D) 5-YHEDA-immunocolloidal gold particles were detected around the brain blood vessels of the bs-5-YHEDA–injected SN mouse. The surrounding iron clustered and colocalized with bs-5-YHEDA oligomers. In contrast, in the brain treated with 5-YHEDA, gold particles could not be observed, and the surrounding iron was denser. Abbreviations: BBB, blood-brain barrier; LDLR, low-density lipoprotein receptor.

3.4. bs-5-YHEDA can bind LDLR and thus cross the BBB to enter the brain

The coimmunoprecipitation assay demonstrated that bs-5-YHEDA can bind to LDLR. As shown in lane 3 in Fig. 4A, above LDLR, at the molecular weight of approximately 100 kDa, there is a bold black band, which is equal to the sum weight of bs-5-YHEDA and LDLR, suggesting that bs-5-YHEDA was bound by the LDLR and thus coprecipitated. In contrast, when the binding segment–lacking 5-YHEDA was mixed with LDLR, the mixture only electrophoresed two thick bands: a bold band located at the same level as LDLR, and the other light band ran to the bottom, with blurry strips closed to each (which might indicate other trace molecule affinity to LDLR or 5-YHEDA). In lane 5, no band was observed thicker than the 100 kDa band of lane 3, suggesting that the 5-YHEDA, if lacking the binding segment, seldom will interact with LDLR.

Fig. 4B-c shows that the LDLR-binding segment linking enabled the cardiac-injected therapeutic 5-YHEDA peptide to enter the brain. The bs-5-YHEDA peptides were observed to be immunohistochemically stained brown and scattered in the brain slices. In contrast, in the brain sections from mice intracardially injected with only 5-YHEDA, no staining was

observed (Fig. 4B-b). The ^{3}H-autoradiography further demonstrated that after 6 days of cardiac injection of 200 μL 20 μM ^{3}H-bs-5-YHEDA, the concentration of the remaining ^{3}H-bs-5-YHEDA in the CSF was approximately 0.26 μM, which is still an active concentration (Fig. 4C-b).

A colloidal gold immunoassay further demonstrated that in the SN mouse brain the cardiac-injected bs-5-YHEDA peptide bound iron. As a consequence, the iron in the vicinity of bs-5-YHEDA was clustered to colocalize with the peptide but was scarce in the surrounding area (Fig. 4D-c). In contrast, when 5-YHEDA was not linked to the LDLR-binding segment, the gold particles were not observed in the brain, and the background iron was denser (Fig. 4D-b). Thus, it is plausible that without the aid of the LDLR-binding segment, it is difficult for 5-YHEDA to cross the BBB and enter the brain.

3.5. bs-5-YHEDA might protect the brain and improve the cognitive status of SN mice

Dose and duration-effect investigations demonstrated that with increasing concentrations, the iron and hydroxyl radicals in CSF decreased. When the concentration increased to 5 μM, and after 4 weekly cardiac injections of 200 μL bs-5-YHEDA,
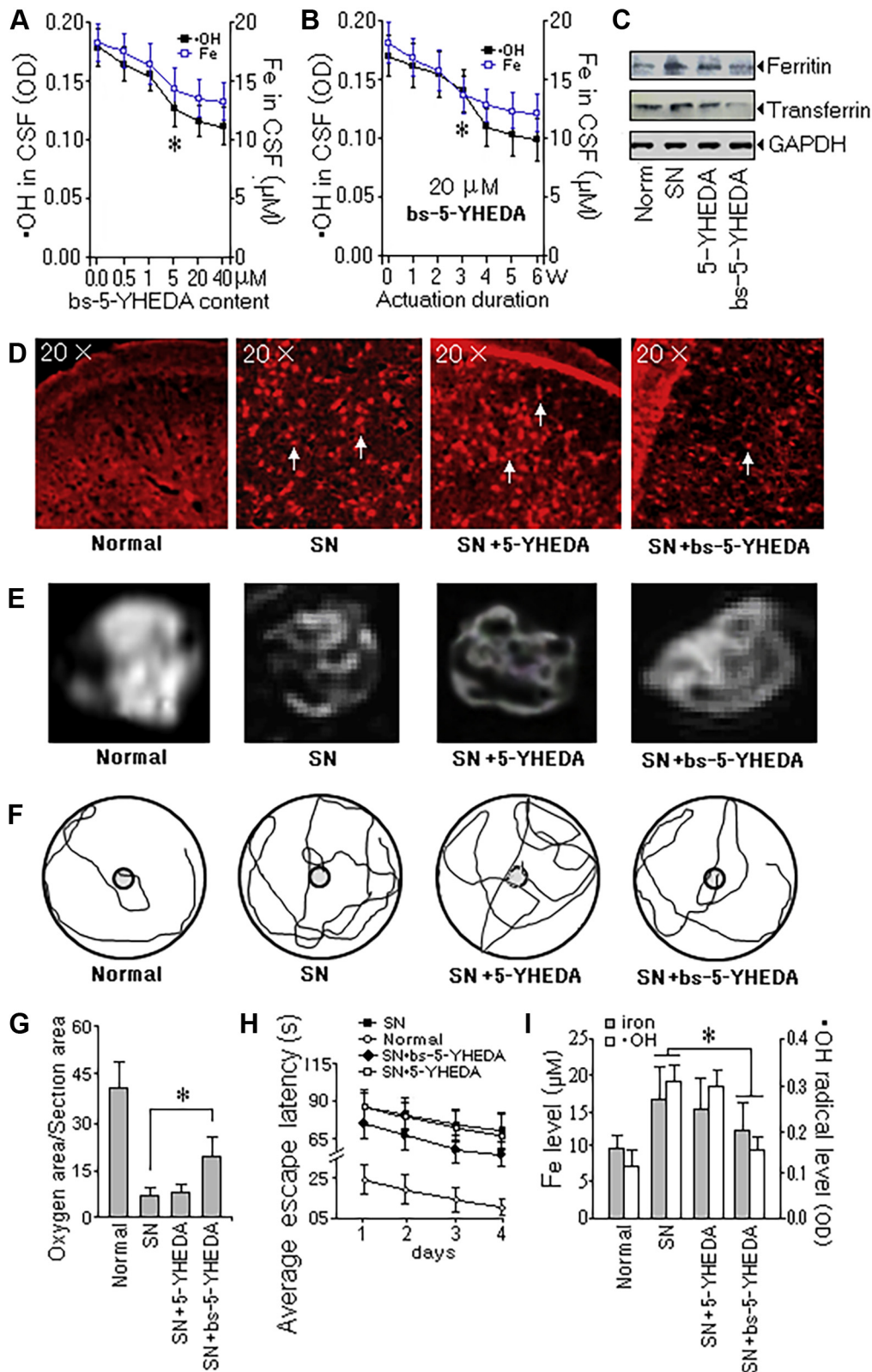
Fig. 5. The iron and radicals in the brains of SN mice were scavenged by LDLR-mediated endocytosed bs-5-YHEDA; thus, neuronal necrosis and cognitive deterioration were retarded. To evaluate the efficiency of 5-YHEDA in protecting the brain, or even more, stop the cognition of SN mouse deterioration, the LDLR-binding segment was linked to 5-YHEDA and intracardially injected into SN mice. (A) Pretreatment, a dose-effect investigation was performed, and the results showed that a dose of more than 5.0 μM significantly decreased the content of hydroxyl radicals in the SN brain, whereas the brain iron decreased along with the density of bs-5-YHEDA. However, when the density exceeded 20 μM, the effect of radical scavenging slowed. (B) After 3 weeks of 20 μM bs-5-YHEDA cardiac injection, the level of hydroxyl radical decreased to 0.13 optical density, and prolonging the bs-5-YHEDA administration shows little effect on radical decrease. (C) With aging, the brain ferritin and transferrin increased in the senile mice. However, in the brains of SN mice treated with bs-5-YHEDA,

Table 1
Clinical chemistry and blood index tests

Organ	Index	Normal	bs-5-YHEDA	SN	SN + bs-5-YHEDA	RRs [33,34]
Liver	ALT (IU/L)	81 ± 8	73 ± 7	159 ± 9↑	178 ± 18↑	54–242
	AST (IU/L)	43 ± 7	50 ± 6	85 ± 8↑	92 ± 5↑	26–70
Kidney	SCr (mg/dL)	0.48 ± 0.02	0.51 ± 0.05	0.67 ± 0.06	0.58 ± 0.07	0.30–1.00
	BUN (mg/dL)	16.8 ± 2.3	18.6 ± 2.1	17.1 ± 0.9	19.6 ± 1.5	13.9–28.3
Blood	RBC count (10^6 count/µL)	6.6 ± 0.8	7.6 ± 0.7↑	4.3 ± 0.5↓	8.7 ± 0.8↑ ▲	
	MCV (fL)	45.9 ± 2.3	46.5 ± 3.0	46.8 ± 6.2	48.4 ± 5.4	
	RDW (%CV)	24.3 ± 2.6	24.6 ± 3.1	25.6 ± 3.9	26.9 ± 4.5↑	
	HCT (%)	29.3 ± 1.7	36.7 ± 2.5↑	21.8 ± 3.1↓	41.5 ± 5.7↑ ▲	
	MCHC (g/L)	34.2 ± 2.1	34.8 ± 1.5	29.8 ± 2.9↓	36.1 ± 2.5▲	
	WBC count (10^3 count/µL)	9.0 ± 1.7	9.1 ± 1.3	9.1 ± 1.6↑	9.3 ± 1.5↑	
	NE (%)	17.8 ± 3.0	18.1 ± 2.8	18.5 ± 3.6	17.7 ± 3.4	
	EO (%)	2.7 ± 0.4	2.7 ± 0.4	2.9 ± 0.7↑	2.4 ± 0.6↓ ▼	
	BA (%)	2.0 ± 0.4	2.2 ± 0.5	2.3 ± 0.5	2.4 ± 0.6↑	
	LY (%)	84.2 ± 3.2	85.7 ± 3.0	97.3 ± 2.8↑	91.2 ± 0.8↑ ▼	
	MO (%)	3.7 ± 0.4	3.8 ± 0.5	7.7 ± 0.6↑	7.8 ± 0.5↑	
	PLT count (10^3 count/µL)	748 ± 84	737 ± 90	582 ± 58↓	722 ± 51↓ ▼	
	MPV (fL)	6.8 ± 0.9	6.7 ± 1.0	7.6 ± 1.3↑	7.4 ± 0.7↑	

NOTE. ↑: Compared with the normal mouse; ▲ ▼: compared with the SN mouse. $P < 5\%$.

Abbreviations: ALT, alanine transaminase; AST, aspartate aminotransferase; BA, basophil percentage; BUN, blood urea nitrogen; EO, eosinophil percentage; HCT, hematocrit; LY, lymphocyte percentage; MCH, mean corpuscular hemoglobin; MCHC, mean corpuscular hemoglobin concentration; MCV, mean corpuscular volume; MO, monocyte percentage; MPV, mean platelet volume; NE, neutrophil percentage; PLT, platelet; RBC, red blood cell; RDW, red cell distribution width; RRs, reference ranges; SCr, serum creatinine; SN, senescent; WBC, white blood cell.

the hydroxyl radicals of the in vivo CSF significantly decreased to 0.12 optical density; moreover, the CSF iron concentration decreased to 12 µM from 18 µM (Fig. 5A). After three times of a weekly administration of 200 µL of 20 µM bs-5-YHEDA, the hydroxyl radical in the CSF decreased to 0.13 in optical density, and the CSF iron decreased to 13 µM; after the fourth week, the radical decreased slowly (Fig. 5B). In the regular experiments, we treated the mice with 200 µL of 20 µM bs-5-YHEDA each time.

From Fig. 5C, we know that, with aging, the brain iron storage protein ferritin in SN mice increased by 60% and the iron-internal transportation protein transferrin increased by 30% on average after age 6 months. However, when the SN mice were treated with bs-5-YHEDA for approximately 6 weeks, the increased brain ferritin and transferrin reversed, suggesting that bs-5-YHEDA can prevent brain iron level enhance by abating the accumulation and reduced the intracerebral transportation. As a result, the neurons in the SN brain displayed less disorder and less necrosis (the bright spots pointed by arrow in Fig. 5D are the necrotic neurons) than those in the untreated SN mice (Fig. 5D), that is, bs-5-YHEDA protected the neurons by shunting the iron-catalyzed radical attack. In contrast, in the brains of mice treated with the binding segment–lacking 5-YHEDA, the aforementioned effects were not observed; in these mice, the iron and radical

levels in the brain were nearly the same as those in the untreated SN mice (Fig. 5I).

Furthermore, after the bs-5-YHEDA treatment, we observed that, compared with that in the untreated SN mice, the brain blood oxygen metabolism level (bright areas in the brain shown in Fig. 5E, and counted in chart Fig. 5G) was 82% higher. The MWM (Fig. 5F and H) showed that after the training, the bs-5-YHEDA–treated SN mice were less clumsy than the untreated SN mice and the SN mice treated with 5-YHEDA. The bs-5-YHEDA–treated SN mice took only 57 seconds on average and swam 220 cm to return to the hidden platform in the MWM, nearly 25 seconds faster and 90 cm less than the untreated mice and the 5-YHEDA–treated SN mice (Fig. 5F and H), which suggests that the synthesized bs-5-YHEDA peptide prevented the deterioration of cognition and memory in the mice. Without the binding segment, it is difficult for the 5-YHEDA peptide to enter the brain, much less scavenging the brain iron and radicals.

3.6. The side effects on liver, kidney, and blood were not observed in bs-5-YHEDA–treated mice; instead, bs-5-YHEDA relieved senescence-induced inflammation

A good medicine should not only have a high curative efficacy but also cause no side effects in the body. To determine

their levels were reversed. (D) The brains of untreated SN mice were widely distributed with necrotic neurons. The 5-YHEDA peptide did not prevent neuronal damage, and the necrotic neurons in the brain were still as many as those in the untreated SN mice. However, if the bs-5-YHEDA was delivered, the neuron necrosis in the SN mouse was slowed down; (E and G) consequently, the blood oxygen in the SN brain did not decline as quickly as that in the untreated SN or 5-YHEDA–injected SN mice, and the active brain area remained nearly 82% wider than that in the two groups aforementioned. (F and H) The MWM test demonstrated that the bs-5-YHEDA–treated SN mice swam less time than the untreated SN and 5-YHEDA–treated SN mice to find the underwater stage. (I) The iron and radical assay showed that bs-5-YHEDA greatly retarded the brain iron and hydroxyl radical accumulations in the SN mice. $*P < .05$.
Abbreviations: CSF, cerebrospinal fluid; LDLR, low-density lipoprotein receptor; MWM, Morris water maze; SN, senescent.

whether bs-5-YHEDA yields adverse effects, liver and kidney chemistry and whole blood tests were performed after bs-5-YHEDA treatment. As shown in Table 1, the alanine aminotransferase and aspartate aminotransferase levels increased nearly twofold in the process of aging, and although bs-5-YHEDA did not reverse the senescence-induced liver injury, it did not aggravate the seriousness. Neither bs-5-YHEDA nor aging exerted a significant adverse effect on the kidney. The creatinine in the serum and blood urea nitrogen levels in the SN mice and the bs-5-YHEDA–treated mice were nearly the same as those of the control, implying that bs-5-YHEDA will not harm kidneys.

Senescence and the bs-5-YHEDA treatment had little influence on the mean corpuscular volume or percentage of neutrophils, and the bs-5-YHEDA treatment caused little change in the senescence-related increases in the red cell distribution width and monocyte percentage. However, the bs-5-YHEDA treatment reversed the senescence-induced decreases in the red blood cell count, hematocrit, platelet count, and mean corpuscular hemoglobin concentration in the mice. Likewise, the increased lymphocyte percentage, mean platelet volume, and eosinophil percentage in the SN mice were reversed after bs-5-YHEDA administration, suggesting that bs-5-YHEDA has an anti-inflammatory effect and can partially alleviate anemia.

4. Discussion

AD has a profound impact on patients as well as their families and friends. However, the pathogenesis of this disease is not yet fully understood.

Possibly in part because of changes in the levels of iron-metabolic proteins throughout the development process, such as the increase in iron-conserving ferritin and iron-internal transporting transferrin, iron accumulates locally in the brain [35–37] and acts as a fundamental catalyzer of free radicals. The bivalent form of iron, Fe^{2+}, is capable of transferring one electron to O_2, producing the superoxide radical $\bullet O_2^-$. The reaction of Fe^{2+} with H_2O_2 produces the highly reactive hydroxyl radical ($\bullet OH$) [6]. These oxygen free radicals, plus H_2O_2 and singlet oxygen, may imperil neurons in iron-rich regions [7]. Therefore, iron can be regarded as an important pathophysiological element for AD.

Some iron-removing agents, such as DFO, deferasirox (DFX), and DFP, have been used clinically to remove iron from tissues [8–11,38]. DFO causes the excretion of iron in urine by binding iron to form water-soluble ferrioxamine; DFX removes iron from the blood and tissues by chelating iron atoms; DFP is orally active and smaller than DFO, thus enabling DFP to cross the BBB to chelate the excess iron in the brain [8–11,38]. Nevertheless, there are numerous side effects of these treatments on organisms. An overdose of DFO (>50 mg/kg body weight) is damaging to the pulmonary, sensorimotor, renal, auditory, and ocular systems [39] and hinders growth [40]. DFP causes agranulocytosis, arthralgia, zinc deficiency, and dia-

betes [41], and without exception, DFX gives rise to headaches, nausea, vomiting, and joint pain [42]; such side effects greatly limit the use of these agents. Thus, identifying a nontoxic iron chelator is important for treating AD or iron-associated diseases.

The polar amino acids Tyr (Y), His (H), Glu (E), and Asp (D) are the amino residues in the $A\beta_{42}$ peptide with affinity for iron. To chelate the excess iron in the brains of SN mice, we combined these amino acids and synthesized an oligomer composed of the Y-H-E-D-A residues. Compared with $A\beta_{42}$, this oligomer is not only soluble in water and CSF but also has more iron-binding residues and thus a higher affinity for iron (Figs. 2B-d, C-b, D-b and 4C-c). Accordingly, this peptide is competitive in radical clearance (Figs. 3B, E and 5A, B, I).

However, the BBB, which is formed by endothelial cell tight junctions in blood vessel walls, severely hampers drug delivery [24]; agents >500 Da cannot pass the barrier to reach the brain. Although the 5-YHEDA peptide has an affinity for iron, its large molecular size (3574.5 Da) hampers its passage across the BBB, greatly limiting its iron-scavenging effect. We thus considered alternative approaches, including receptor- or transporter-mediated delivery, which transfer essential substances such as glucose, insulin, growth hormone, and low-density lipoprotein, among others [43]. By conjugating the LDLR-binding domain of ApoB-100 to our therapeutic 5-YHEDA (abbreviated as bs-5-YHEDA), we enabled it to be recognized and bound by cerebral vascular endothelial cells, and then we delivered the bs-5-YHEDA into the iron-rich brain of the SN mouse via LDLR-mediated transcytosis after intracardiac injection. The bs-5-YHEDA that entered the brain functioned in an iron-scavenging role, possibly not only by directly chelating iron at residues His, Tyr, Glu or, Asp [44] but also by the mechanism unknowing way of decreasing the absorption through reversing the increase in ferritin and the transferrin in aging mice (Fig. 5C), which reduced the radical catalysis and the subsequent neuronal injury (Fig. 5). Accordingly, the cognitive status of the mice showed less impairment by senescence compared with that of the untreated SN mice. Because of the radical catalysis reduction, senescence-related anemia and inflammation (which is also a pathogeny for AD [45]) were reversed without kidney injury (Table 1). In addition, side effects such as diarrhea, vomiting, fever, and gastrointestinal hemorrhage, which commonly occur in patients taking DFO, DFP, or DXO, were not observed in the bs-5-YHEDA–treated mice.

Nevertheless, for bs-5-YHEDA to become a new ligand of LDLR, problems such as whether it competes with other LDLR substrates such as ApoE or ApoB, thus crippling the endocytosis, transport, and degradation of lipids, must be addressed. As pointed out by Coleman et al. [46] and Devaraj and Jialal [47], ApoB is a 510 kDa molecule, and ApoE is as large as 34 kDa [48]; both substrates are beyond the scale of

our Western blot ruler if forming complexes with LDLR (93 kDa). Indeed, there are weak compounds exceeded the maximum scale of 120 kDa, ApoB or ApoE binding was not excluded. $A\beta_{42}$ per se can also bind ApoE, and by LDLR-mediated endocytosis, $A\beta_{42}$ is either carried to lysosomes and scavenged or aggregated in the brain, forming senile plaques after binding to ApoE, which aggravates AD [48]. Furthermore, if bs-5-YHEDA, as a ligand of LDLR, wins the competition with ApoE to bind LDLR, this may weaken the clearance of $A\beta_{42}$. A plethora of reports have claimed that the agglomeration of $A\beta_{42}$ in the brain poses a pathogeny to AD. Will our bs-5-YHEDA bind $A\beta_{42}$ to form aggregation, thus aggravating AD? As Pillot illustrated, the binding sites in ApoE are the residues capable of forming disulfide bonds, such as cysteine and methionine located at the carboxy-terminal domain 244 to 272: EEQTQ-QIRLQAEIFQARLKGWFEPIVEDM. The sulfoxidation of the site-specific methionine renders ApoE capable of binding $A\beta_{42}$ [49,50]. Our bs-5-YHEDA: YHEDAYHEDAYHE-DAYHEDAYHEDA QSDIVAHLL, lacks methionine and cysteine residues. However, $A\beta_{42}$: DAEFRHDSGYEVH-HEKLVF FAEDVGSNKGAIIGLMVGGVVIA has methionine$_{35}$. There is the risk that the two peptides would interact or the $A\beta_{42}$ fibrils would self-aggregate to form an agglomeration. Indeed, the transmission electron microscope images in Supplementary Fig. 1A show that there were crispated fibrils overlapping each other in the incubated synthesized $A\beta_{42}$:bs-5-YHEDA mixture, and different bands (stained by 1% Coomassie brilliant blue) were electrophoresed in the incubated $A\beta_{42}$ lane or in the incubated $A\beta_{42}$:bs-5-YHEDA mixture lane (Supplementary Fig. 1B). However, the bs-5-YHEDA band in the $A\beta_{42}$:bs-5-YHEDA mixture lane had nearly the same density as that in the bs-5-YHEDA-only lane, suggesting that no bs-5-YHEDA was expropriated to combine $A\beta_{42}$. Therefore, the bs-5-YHEDA peptide may not promote the aggregation of $A\beta_{42}$ to aggravate AD. In contrast, it might be a safer and milder iron remover in the clinic that is capable of crossing the BBB to scavenge excessive iron in the brain, thus reducing the catalyzed radicals and retarding the senescence process. However, the human body is a complex system. If bs-5-YHEDA is adopted, its effectiveness will be affected by many factors. Despite that, we are still conducting trials to seek a low-cost technology to use this peptide to relieve patients affected by iron and radical diseases such as AD.

Acknowledgments

Declarations: The animal experiments were performed in strict accordance with the Guidance for the Care and Use of Laboratory Animals of the National Institutes of Health, and the protocol was approved by the Committee on the Ethics of Animal Experiments of Taizhou University (Permit Number: 15-1523).

Supplementary Data

Supplementary data related to this article can be found at https://doi.org/10.1016/j.trci.2019.07.013.

RESEARCH IN CONTEXT

1. Systematic review: The authors reviewed the pathology of iron in Alzheimer's disease and summarized some iron removers and the methods to deliver macromolecular crossing the blood-brain barrier.

2. Interpretation: In the study, the authors designed an iron-affinitive peptide bs-5-YHEDA. By connecting it with a low-density lipoprotein receptor binding segment, the peptide crossed the blood-brain barrier via and entered into the brain of senescent mice low-density lipoprotein receptor-mediated endocytosis, where scavenged the free iron and reduced the catalyzed free radicals, with the result of brain protecting and cognitive decline alleviating.

3. Future directions: In the future, the authors will do experiments to explore how the bs-5-YHEDA regulates the expression of ferritin, transferrin, and hepcidin to reduce brain iron, and plan to have a clinical trial with the view of to relieve the patients' suffering.

References

[1] Querfurth HW, LaFerla FM. Alzheimer's disease. N Engl J Med 2010; 362:329–44.

[2] Tiraboschi P, Hansen LA, Thal LJ, Corey-Bloom J. The importance of neuritic plaques and tangles to the development and evolution of AD. Neurology 2004;62:1984–9.

[3] Thompson CA, Spilsbury K, Hall J, Birks Y, Barnes C, Adamson J. Systematic review of information and support interventions for caregivers of people with dementia. BMC Geriatr 2007;7:18.

[4] Gumienna-Kontecka E, Pyrkosz-Bulska M. Iron chelating strategies in systemic metal overload, neurodegeneration and cancer. Curr Med Chem 2014;21:3741–67.

[5] Hardy J, Allsop D. Amyloid deposition as the central event in the aetiology of Alzheimer's disease. Trends Pharmacol Sci 1991;12:383–8.

[6] Mudher A, Lovestone S. Alzheimer's disease-do tauists and baptists finally shake hands? Trends Neurosci 2002;25:22–6.

[7] Ward RJ, Zucca FA, Duyn JH, Crichton RR, Zecca L. The role of iron in brain ageing and neurodegenerative disorders. Lancet Neurol 2014; 13:1045–60.

[8] Liu G, Men P, Perry G, Smith MA. Nanoparticle and iron chelators as a potential novel Alzheimer therapy. Methods Mol Biol 2010; 610:123–44.

[9] McLachlan DR, Kruck TP, Lukiw WJ, Krishnan SS. Would decreased aluminum ingestion reduce the incidence of Alzheimer's disease? CMAJ 1991;145:793–804.

[10] Cuajungco MP, Faget KY, Huang X, Tanzi RE, Bush AI. Metal chelation as a potential therapy for Alzheimer's disease. Ann NY Acad Sci 2000;920:292–304.

[11] Richardson DR, Ponka P. Development of iron chelators to treat iron overload disease and their use as experimental tools to probe intracellular iron metabolism. Am J Hematol 1998;58:299–305.

[12] Kontoghiorghes GJ. New concepts of iron and aluminium chelation therapy with oral L1 (deferiprone) and other chelators. A review. Analyst 1995;120:845–85.

[13] Crowe A, Morgan EH. Effects of chelators on iron uptake and release by the brain in the rat. Neurochem Res 1994;19:71–6.

[14] Gassen M, Youdim MB. The potential role of iron chelators in the treatment of Parkinson's disease and related neurological disorders. Pharmacol Toxicol 1997;80:159–66.

[15] Bergeron RJ, Brittenham GM. The Development of Iron Chelators for Clinical Use. Boca Raton: CRC; 1994. p. 353–71.

[16] Galanello R, Campus S. Deferiprone chelation therapy for thalassemia major. Acta Haematol 2009;122:155–64.

[17] Levy M, Llinas RH. Deferiprone reduces hemosiderin deposits in the brain of a patient with superficial siderosis. AJNR Am J Neuroradiol 2011;32:E1–2.

[18] Vivekanandan S, Brender JR, Lee SY, Ramamoorthy A. A partially folded structure of amyloid-beta (1-40) in an aqueous environment. Biochem Biophysical Res Commun 2011;411:312–6.

[19] Bousejra-ElGarah F, Bijani C, Coppel Y, Faller P, Hureau C. Iron (II) binding to amyloid-β, the Alzheimer's peptide. Inorg Chem 2011; 50:9024–30.

[20] Atwood CS, Scarpa RC, Huang X, Moir RD, Jones WD, Fairlie DP. Characterization of copper interactions with Alzheimer amyloid beta peptides: identification of an attomolar-affinity copper binding site on amyloid beta1-42. J Neurochem 2000;75:1219–33.

[21] Zhang W, Johnson BR, Suri DE, Martinez J, Bjornsson TD. Immunohistochemical demonstration of tissue transglutaminase in amyloid plaques. Acta Neuropathol 1998;96:395–400.

[22] Zou K, Gong JS, Yanagisawa K, Michikawa M. A novel function of monomeric amyloid beta-protein serving as an antioxidant molecule against metal-induced oxidative damage. J Neurosci 2002; 22:4833–41.

[23] Baruch-Suchodolsky R, Fischer B. Aβ40, either soluble or aggregated, is a remarkably potent antioxidant in cell-free oxidative systems. Biochemistry 2009;48:4354–70.

[24] Sarkar G, Curran GL, Mahlum E, Decklever T, Wengenack TM, Blahnik A, et al. A carrier for non-covalent delivery of functional beta-galactosidase and antibodies against amyloid plaques and IgM to the brain. PLoS One 2001;6:e28881.

[25] Deane R, Sagare A, Hamm K, Parisi M, LaRue B, Guo H, et al. IgG-assisted age dependent clearance of Alzheimer's amyloid beta peptide by the blood-brain barrier neonatal Fc receptor. J Neurosci 2005; 25:11495–503.

[26] Jefferies WA, Brandon MR, Hunt SV, Williams AF, Gatter KC, Mason DY. Transferrin receptor on endothelium of brain capillaries. Nature 1984;312:162–3.

[27] Zlokovic BV, Jovanovic S, Miao W, Samara S, Verma S, Farrell CL. Differential regulation of leptin transport by the choroid plexus and blood-brain barrier and high affinity transport systems for entry into

hypothalamus and across the blood-cerebrospinal fluid barrier. Endocrinology 2000;141:1434–41.

[28] Gabathuler R. Approaches to transport therapeutic drugs across the blood–brain barrier to treat brain diseases. Neurobiol Dis 2010; 37:48–57.

[29] Brian JS, Inder MV. Targeted delivery of proteins across the blood–brain barrier. Proc Natl Acad Sci U S A 2007;104:7594–9.

[30] Jere PS, Martin KJ, Hans De L, Nassrin D. Structure of apolipoprotein B-100 in low density lipoproteins. J Lipid Res 2001;42:1346–67.

[31] George P, Charles W. The Rat Brain in Stereotaxic Coordinates, Compact. 6th ed. San Diego, London, Boston, New York Sydney, Tokyo, Toronto: Academic Press; 2008.

[32] Solberg HE, International Federation of clinical chemistry. Scientific Committee, clinical section. Expert panel on theory of reference values and International Committee for Standardization in Haematology Standing Committee on reference values. Approved recommendation on the theory of reference values. Part 1. The concept of reference values. Clin Chim Acta 1987;165:111–8.

[33] Mazzaccara C, Labruna G, Cito G, Scarfò M, De Felice M, Pastore L, et al. Age-related reference intervals of the main biochemical and hematological parameters in C57BL/6J, 129SV/EV and C3H/HeJ mouse strains. PLoS One 2008;3:e3772.

[34] Harrill AH, Desmet KD, Wolf KK, Bridges AS, Eaddy JS, Kurtz CL, et al. A mouse diversity panel approach reveals the potential for clinical kidney injury due to DB289 not predicted by classical rodent models. Toxicol Sci 2012;130:416–26.

[35] Raha AA, Vaishnav RA, Friedland RP, Bomford A, Raha-Chowdhury R. The systemic iron-regulatory proteins hepcidin and ferroportin are reduced in the brain in Alzheimer's disease. Acta Neuropathol Commun 2013;3:55.

[36] Thomas W, Christos M, Antigoni E, Kalotina G, Harold GP, Maria S, et al. Dissociation between iron accumulation and ferritin upregulation in the aged substantia nigra: attenuation by dietary restriction. Aging (Albany, NY) 2016;8:2488–506.

[37] Fernández T, Martínez-Serrano A, Cussó L, Desco M, Ramos-Gómez M. Functionalization and characterization of magnetic nanoparticles for the detection of ferritin accumulation in Alzheimer's disease. ACS Chem Neurosci 2018;9:912–24.

[38] Malik A, Firke SD, Patil RR, Shirkhedkar AA, Surana SJ. Determination of iron chelating agents by analytical methods: a review. Crit Rev Anal Chem 2019;29:1–11.

[39] Brittenham GM, Olivieri NF. Iron-chelating therapy and the treatment of thalassemia. J Am Soc Hematol 1997;89:739–61.

[40] Olivieri NF, Koren G, Harris J, Khattak S, Freedman MH, Templeton DM, et al. Growth failure and bony changes induced by deferoxamine. J Pediatr Hematol Oncol 1992;14:48–56.

[41] Wiwanitkit V. Quantum chemical analysis of the deferiprone-iron binding reaction. Int J Nanomedicine 2006;1:111–3.

[42] How are thalassemias treated? National Heart, Lung, and Blood Institute, 2013. https://www.nih.gov/about-nih/what-we-do/nih-almanac/national-heart-lung-blood-institute-nhlbi. Accessed September 6, 2019.

[43] Pardridge WM. Blood–brain barrier delivery. Drug Discov Today 2007;12:54–61.

[44] Zou Z, Cai J, Zhong A, Zhou Y, Wang Z, Wu Z, et al. Using the synthesized peptide HAYED (5) to protect the brain against iron catalyzed radical attack in a naturally senescence Kunming mouse model. Free Radic Biol Med 2019;130:458–70.

[45] Abbott A. Is 'friendly fire' in the brain provoking Alzheimer's disease? Nature 2018;556:426–8.

[46] Coleman RA, Haynes EB, Sand TM, Davis RA. Developmental coordinate expression of triacylglycerol and small molecular weight apoB synthesis and secretion by rat hepatocytes. J Lipid Res 1988; 29:33–42.

[47] Devaraj S, Jialal I. Biochemistry, Apolipoprotein B. StatPearls [Internet]. Treasure Island (FL): StatPearls Publishing; 2019.

[48] Zhao N, Liu C-C, Qiao W, Bu G. Apolipoprotein E, receptors, and modulation of Alzheimer's disease. Biol Psychiatry 2018; 83:347–57.

[49] Strittmatter WJ, Weisgraber KH, Huang DY, Dong LM, Salvesen GS, Pericak-Vance M, et al. Binding of human apolipoprotein E to synthetic amyloid beta peptide: isoform-specific effects and implications for late-onset Alzheimer disease. Proc Natl Acad Sci U S A 1993; 90:8098–102.

[50] Pillot T, Goethals M, Najib J, Labeur C, Lins L, Chambaz J, et al. β-Amyloid peptide interacts specifically with the carboxy-terminal domain of human apolipoprotein E: relevance to Alzheimer's disease. J Neurochem 1999;72:230–7.